CrossMark

Super-resolution imaging by microsphere-assisted optical microscopy

Qiaowen Lin[1,2] · Dayong Wang[1] · Yunxin Wang[1] ·
Lu Rong[1] · Jie Zhao[1] · Sha Guo[1] · Minchao Wang[1]

Abstract Microsphere-assisted optical microscopy achieved the nano-scale resolution for the imaging. Some parts of evanescent waves produced by nano-structures can be transformed into propagating waves with the help of microsphere. In this paper, we develop the equations of the resolution and field of view in microsphere imaging system related to the radius and refractive index of microsphere. Through analysis the highest spatial frequency, the resolution reduces quickly with the increase of the radius when the radius is less than 10 μm. The resolution reduces slowly with the increase of the radius when the radius is more than 10 μm. The resolution improves with the increase of refractive index. The size of the focus spot of microsphere is simulated numerically. The simulations are in good agreement with the theoretical prediction about the microsphere-assisted microscopy. Finally, the super-resolution capability of the microsphere has been verified by the experimental results. The results are useful for the practical design of the microsphere-assisted optical microscopy.

Keywords Microscopy · Super-resolution · Microsphere · Evanescent waves

1 Introduction

With the development of nanometer science and life science, the resolution of imaging system is more and more highly demanded in the fields of optical microscopy, photolithography, optical information processing and other optical applications. The sub-wavelength information of sample is carried by evanescent waves which decay

✉ Yunxin Wang
  yxwang@bjut.edu.cn

[1] College of Applied Science, Beijing University of Technology, No. 100 Pingleyuan Rd, Beijing 100124, China

[2] School of Physics and Electronics Science, Shanxi Datong University, Datong 037009, Shanxi, China

exponentially with the distance from the sample. The conventional optical microscopy cannot collect them in the image plane, so the resolution is about $\lambda/2$ by the Abbe diffraction limit of a white light source. How to acquire the evanescent waves and convert them into propagating waves have attracted lots of attention. Many methods have been proposed (Inouye and Kawata 1994; Miklyaev et al. 2014; Pendry 2000; Liu et al. 2006; Jacob et al. 2006; Durant et al. 2006), such as stimulated emission depletion (STED), near-field scanning optical microscopy (NSOM) and far-field super-lenses (FSL). Wang et al. use a SiO_2 microsphere located above a sample to overcome the white light diffraction limit in experiments and obtain the sub-wavelength information imaging of nano-structure (Wang et al. 2011; Li et al. 2013; Lee et al. 2013a, b; Lee and Lin 2015). Hao et al. (2011) use a SiO_2 microsphere semi-immersed in liquid droplet to discern the details of the object whose sizes are below the Abbe diffraction limit. Darafsheh et al. (2012, 2013, 2014, 2015a, b) use a barium titanate glass microsphere with high refractive index immersed in liquids and elastomers to obtain the super-resolution imaging of nano-structures and biological structures . Yan et al. (2014) combined microsphere with laser confocal nanoscope for sub-diffraction-limited imaging at 25 nm lateral resolution in the visible spectrum. In these studies, they illustrate experimentally that microspheres can collect the near-field evanescent waves and transform them into far-field propagating waves. Their samples were usually Blu-Ray DVD disk, fishnet gold-coated anodic aluminum oxide (AAO) membrane star shapes and viruses. Most of people judged the highest resolution through discerning minimal features. For example, when the line width of 100 nm is clearly resolved, the resolution of the imaging system with the white light source ($\lambda = 400$–750 nm) is from $\lambda/4$ to $\lambda/7$. However, Darafsheh et al. (2015a, b) used image deconvolution method to find the FWHM of the PSF as the resolution by using barium titanate glass microspheres. It should be mentioned that the resolution of microsphere-assisted microscopy can be furthermore improved to $\sim\lambda/5.5$ by using a confocal arrangement (Darafsheh et al. 2013, 2014). Ben-Aryeh (2012) theoretically researched evanescent waves from the sample which were transformed into propagating waves with the help of microsphere.

Although he showed a theoretical explanation for the above experiments, it is noticed that acquisition of high resolution and wide field of view are also the key factors for the application fields of microscopy. So we develop the equations of the resolution and field of view in microsphere imaging system related to the radius and refractive index of microsphere. Based on the theoretical analysis, we plot the curve diagrams. They provide the evidence for the improvement of the resolution through selecting the appropriate microsphere during the particular application. The size of the focus spot of microsphere are analyzed further through changing different values of radius and refractive index simulated by the COMSOL Multiphysics based on finite element method. The results are in good agreement with theoretical analysis. The super-resolution capability of the microsphere has been verified by the experimental results.

2 Theoretical analysis of the resolution in the microsphere imaging system

Figure 1 shows a schematic which evanescent waves of the nanostructures through the microsphere illuminated by an incident plane-wave can transform into propagating waves. The contacted point between the microsphere and the sample is O as the origin of

Fig. 1 Schematic of optical field of the nanostructures through the microsphere illuminated by an incident plane-wave
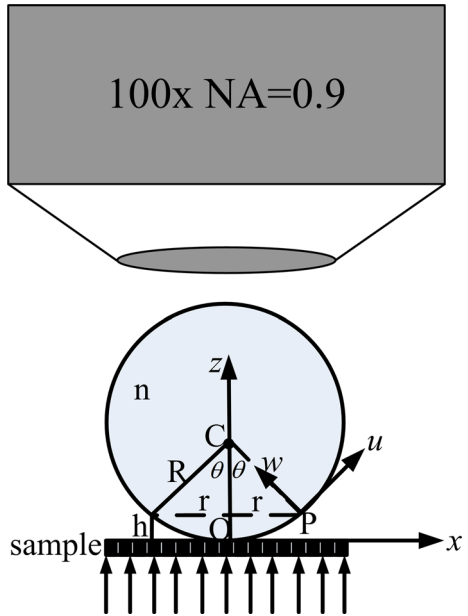
coordinates. C is the center of the microsphere. R is the radius, and n is the refractive index. For simplicity's sake, the plane of $y = 0$ is used to analyze. Let us analyze arbitrary incident point P on edge of the microsphere for example. The vertical distance away from the sample's surface is h. The horizontal distance from O is r. At point P, the vectors of u and w are unit vectors along the tangent direction and normal direction. In air k_0 is divided into $\tilde{k}_u$ and $\tilde{k}_w$ along u and w at the new coordinates. The angle between w and z is θ.

In the microsphere, (k_u, k_w) is the wave vector in the u, w directions, they satisfy the relation

$$k_u^2 + k_w^2 = n^2 k_0^2 \tag{1}$$

After the evanescent wave incident in the microsphere, by Snell's law, the wave vector k_u inside microsphere along u is given by (Ben-Aryeh 2012)

$$k_u^2 = \tilde{k}_u^2 = k_x^2 \cos^2 \theta + k_z^2 \sin^2 \theta = k_x^2 \cos^2 \theta - |k_z|^2 \sin^2 \theta \tag{2}$$

when $k_x^2 \cos^2 \theta - |k_z|^2 \sin^2 \theta > n^2 k_0^2$, the evanescent waves in air propagating in the microsphere are still evanescent waves, they will decay exponentially with the propagating distance. However, when $k_x^2 \cos^2 \theta - |k_z|^2 \sin^2 \theta < n^2 k_0^2$, the evanescent waves become propagating wave.

In above analysis, the microsphere can transform the evanescent waves into propagating waves. To the microscopic imaging system, the resolution and field of view is essential parameters, so in the following part we discuss them. In order to become propagating waves, k_x must meet the following relation

$$k_0^2 \leq k_x^2 \leq \frac{k_0^2(n^2 - \sin^2 \theta)}{1 - 2 \sin^2 \theta} \tag{3}$$

where $\sin \theta \approx \sqrt{2Rh}/R$, it can be expressed as

$$k_0^2 \le k_x^2 \le \frac{k_0^2(n^2 - \sin^2\theta)}{1 - 2\sin^2\theta} = \frac{k_0^2(n^2R - 2h)}{R - 4h} \tag{4}$$

If Y-axis is considered, that $k_y \ne 0$, the arbitrary transverse wave vector $k_{//}$ at the (x, y) plane can be expressed as

$$k_{//}^2 = k_x^2 + k_y^2 \le \frac{k_0^2(n^2R - 2h)}{R - 4h} \tag{5}$$

Let us estimate the highest spatial frequencies f_{max} obtained by microsphere. According to the Eq. (5)

$$f_{max} = \frac{k_{//max}}{2\pi} = \frac{1}{\lambda}\sqrt{\frac{n^2R - 2h}{R - 4h}} \tag{6}$$

The microsphere has spherical symmetries, so it can improve the transverse resolution in all orientations, as described in Fig. 2.

In Fig. 2, the circle area of $f_{//} \le \frac{1}{\lambda}$ expresses propagating waves, and the circle area of $f_{//} > \frac{1}{\lambda}$ expresses evanescent waves. Through the above analysis, the evanescent waves in the circle area defined by $\frac{1}{\lambda} < f_{//} \le \frac{1}{\lambda}\sqrt{\frac{n^2R-2h}{R-4h}}$ can be transformed into propagating wave through the microsphere.

The resolution of microsphere imaging system is expressed as

$$d = \frac{1}{2f_{//max}} = \frac{\lambda}{2}\sqrt{\frac{R - 4\lambda}{n^2R - 2\lambda}} \tag{7}$$

The resolution as function of the radius and refractive index are set up as shown in Fig. 3. The resolution is different as the change of radius and refractive index of microsphere. The resolution reduces quickly with the increase of the radius when the radius is less than 10 μm. The resolution reduces slowly with the increase of the radius when the radius is more than 10 μm. The resolution increases with the increase of refractive index (blue, black and red solid curve). The curves provide a reference for selecting a microsphere.
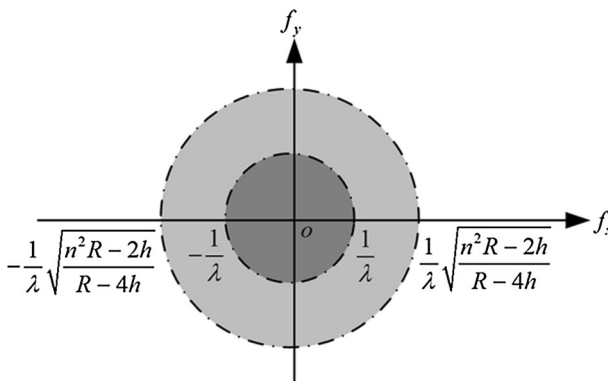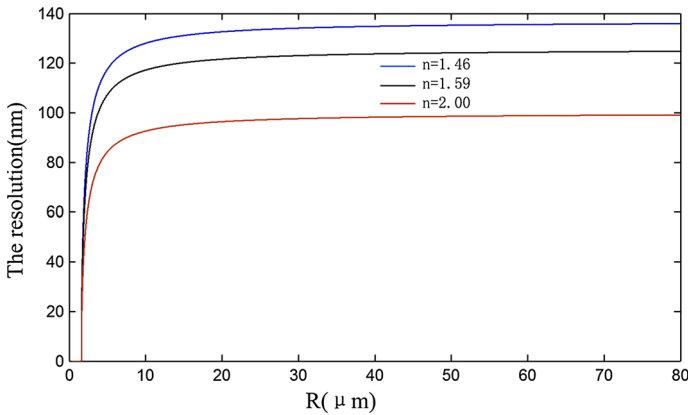

Fig. 2 Microsphere can partly transform the evanescent wave into propagating wave

Fig. 3 The resolution is as a function of the radius and refractive index of the microsphere

Based on Eq. (6), f_{max} as function of h is set up in Fig. 4 when the refractive indexes of microspheres are 1.46, 1.59 and 2.0 respectively. f_{max} increases with the increase of h. The further from the center of a microsphere, the higher obtained frequency.

For the microscopic imaging system, acquisition of high resolution and wide field of view are the goals of our pursuit. The intensity of evanescent wave decays exponentially with the distance away from the interface at which they are formed. Thus the distance between object and microsphere surfaces should be on the same order of magnitude as the wavelength as $h \leq \lambda$, the evanescent waves can be coupled into the microsphere and converted into propagating waves to realize super-resolution. In order to achieve the resolution of the need, we can choose the refractive index and radius of microspheres according to the Fig. 3, so the circle radius of the largest possible field of view can be expressed as follows

$$r = \sqrt{2Rh} \approx \sqrt{2R\lambda} \tag{8}$$

So in order to obtain wide field of view, we can choose a microsphere with higher refractive index and bigger radius according Eq. (7).
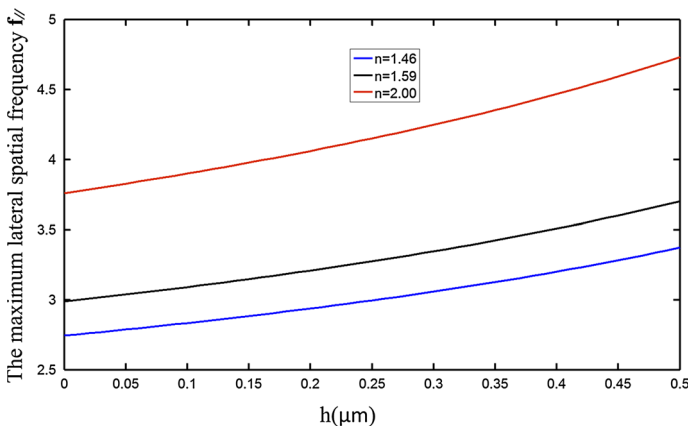
Fig. 4 The correlation between f_{max} and h
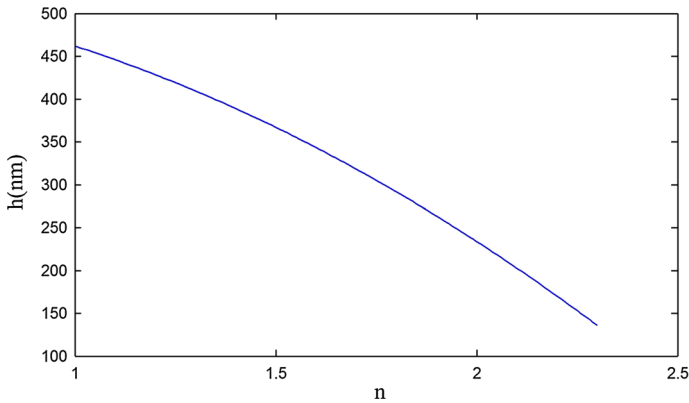
Fig. 5 The correlation between *h* and *n* of the microsphere

In order to achieve a resolution of 100 nm for the radius 2 μm of microsphere, the h as function of *n* is set up in Fig. 5. h decreases with increasing of n. As the resolution of the imaging system linearly increases with the increasing of *n* in the same field of view. For the same radius of microspheres, the bigger refractive index, the obtained frequency is higher in same location.

For a conventional optical microscope, the resolution is limited to about λ/2 because of the loss of evanescent waves during optical wave travelling. The theoretical analysis shows that the resolution can be affected by the radius and refractive index of microspheres. With the help of microsphere, the resolution is smaller than λ/2, so the microsphere can improve the resolution in optical microscope system. The smaller radius and the higher refractive index can get the higher resolution. The results are worthy for selecting the appropriate microsphere.

## 3 Numerical simulations of the focusing properties of the microsphere

In order to verify the theoretical analysis, a full wave simulation using the COMSOL Multiphysics based on finite element method was used to study the properties of the microspheres (Devilez et al. 2008). In simulation, silica (SiO_2) microspheres with the refractive index of 1.46 were illuminated by a plane wave with a wavelength of 400 nm to show the focusing properties of the microspheres with different radius in Fig. 6. The radius of the microspheres were 5, 10, 15, 20 and 25 μm in Fig. 6a–e, respectively. From Fig. 6, we find the maximum intensity in horizontal direction and draw the profiles along the point with maximum intensity in vertical direction as shown in Fig. 6f. The curves are the relations between distance in horizontal direction and intensity with different radius of the microspheres. The simulation results show that the smaller the radius of the microspheres, the smaller the focus spot size and the closer distance from the focus spot to the microspheres. These indicate that the resolution has been improved with the decrease of the radius.

The microspheres with the same radius of 26.5 microns were illuminated by a plane wave with a wavelength of 400 nm to illustrate the focusing properties of the microsphere with different refractive index in Fig. 7. In Fig. 7a, the microsphere is a SiO_2 microsphere with refractive index of 1.46. In Fig. 7b, the microsphere is a polystyrene (PS) microsphere
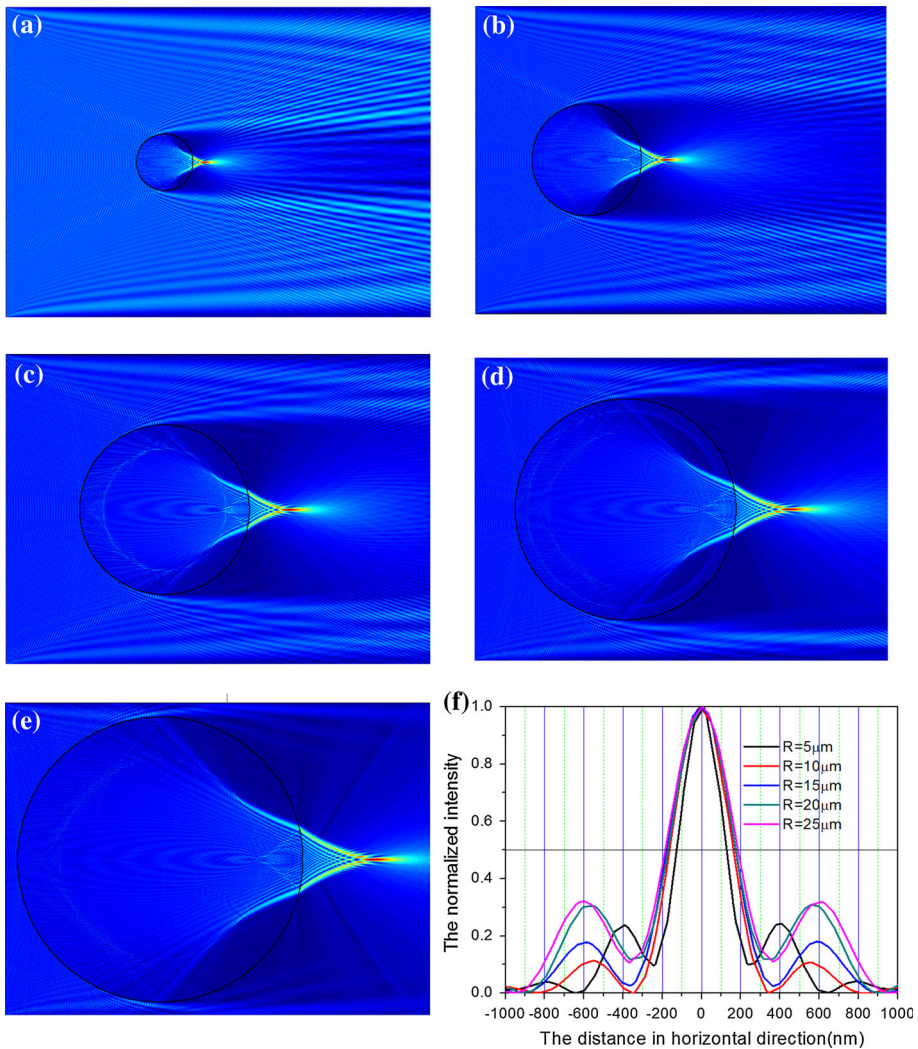
Fig. 6 The simulation of the light propagation through SiO$_2$ microspheres with different radius (**a** R = 5 μm, **b** R = 10 μm, **c** R = 15 μm, **d** R = 20 μm, **e** R = 25 μm) respectively. **f** The simulation results of the light focusing capability of a microsphere, expressed by the FWHM, as a function of the radius of microsphere

with refractive index of 1.59. In Fig. 7c, the microsphere is a Barium titanate (BaTiO$_3$) microsphere with refractive index of 2. The size of spot is less than half of the illumination wavelength in Fig. 7. We find the maximum intensity in horizontal direction and draw the profiles along the point with maximum intensity in vertical direction shown in Fig. 7d. The curves are the relations between distance in horizontal direction and intensity with different refractive indexes of the microspheres. The simulation results show that higher the refractive index of the microspheres, the smaller the focus spot size and the closer distance from the focus spot to the microspheres. These indicate that the resolution has been improved with the increase of the refractive index. By comparing, the simulation results
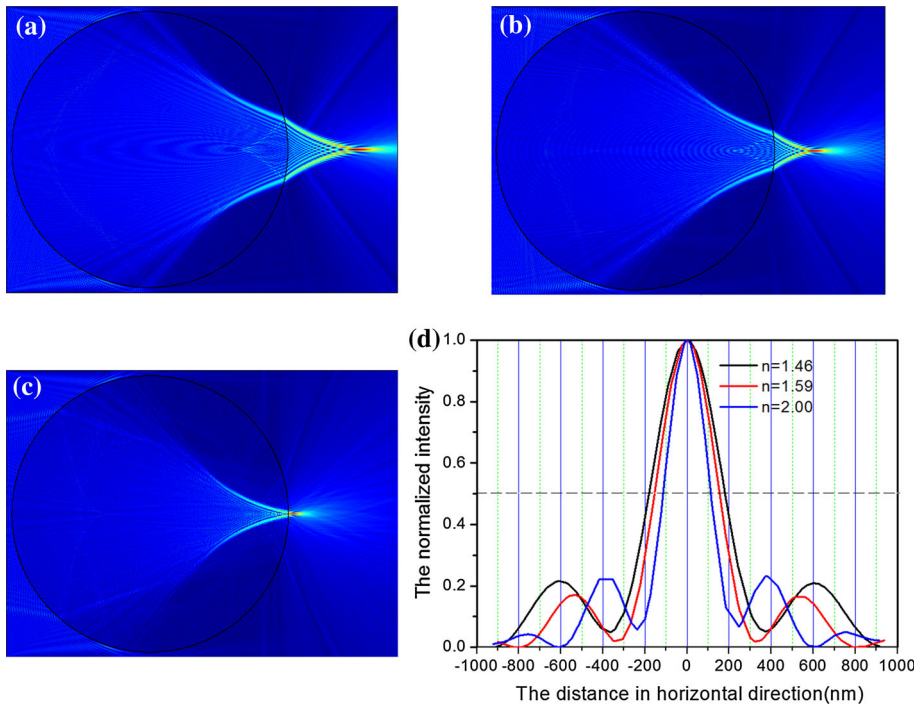
Fig. 7 The simulation of the light propagation through microspheres with different refractive index (**a** n = 1.46, **b** n = 1.59, **c** n = 2) respectively. **d** The simulation results of the light focusing capability of a microsphere, expressed by the FWHM, as a function of the refractive index of microsphere

are consistent with the theoretical derivation and analysis. It is worth noting that the full width at half maximum (FWHM) of the focus spot are larger than the size of the theoretical analysis due to some of the propagating waves inside the microspheres cannot propagate into the air, because they are only located inside the microspheres when total internal reflection occurs.

4 Experimental results

Figure 8 shows the imaging system. The system integrates a microsphere with conventional optical microscopes. The microsphere magnifies the object and forms virtual images by collecting and transforming near-field evanescent waves into propagating waves for super-resolution imaging. Before experiments, the transparent microspheres were placed over the objects. In the experiment, SiO_2 microspheres with 3.6, 25 μm radius and $BaTiO_3$ microspheres with 26.5 μm radius were used. A grating consisting of 140 nm wide lines, spaced 140 nm apart (see Fig. 9), was imaged using an optical microscope (100×, NA = 0.9) with a microsphere under reflection modes. Figure 10a–i are the optical microscopy images obtained by placed SiO_2 microspheres with radius of 3.6 μm (Fig. 10a, d, g), 25 μm (Fig. 10b, e, h) and $BaTiO_3$ microspheres with radius of 26.5 μm (Fig. 10c, f, i) on the grating, respectively. The images of Fig. 10a–c are focused on the center plane of microspheres, so in the images, the grating with nanostructures are out of focus. When the
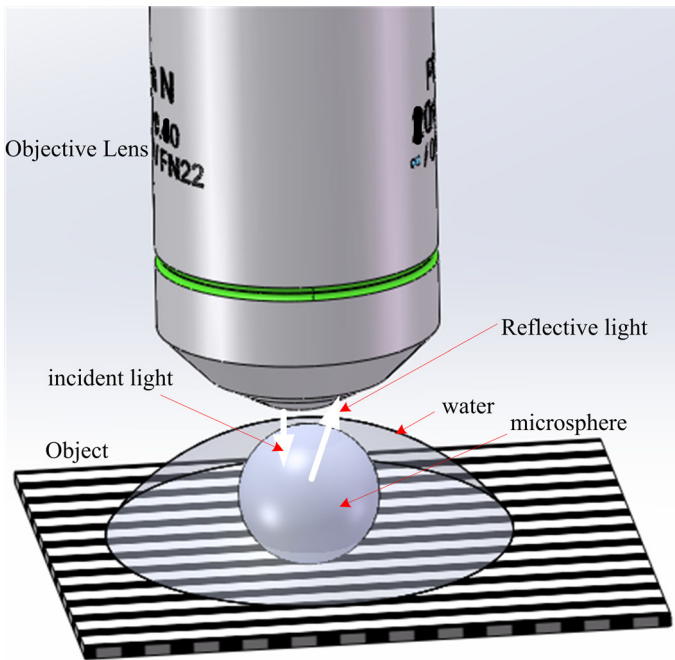
Fig. 8 Schematic of the experimental set-up of microsphere-assisted nanoscope for super-resolution
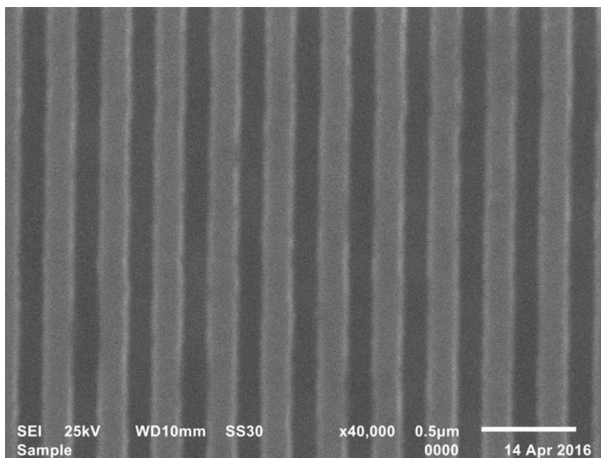
Fig. 9 The image of the grating by SEM

focal plane of the microscope is on the image plane of the microspheres, the corresponding images are shown in Fig. 10d–f respectively. The magnified rectangle area marked with solid blue line in Fig. 10d–f are shown in Fig. 10g–i, respectively. The sub-wavelength information of the grating was observed in Fig. 10d, and it was not observed in Fig. 10e.
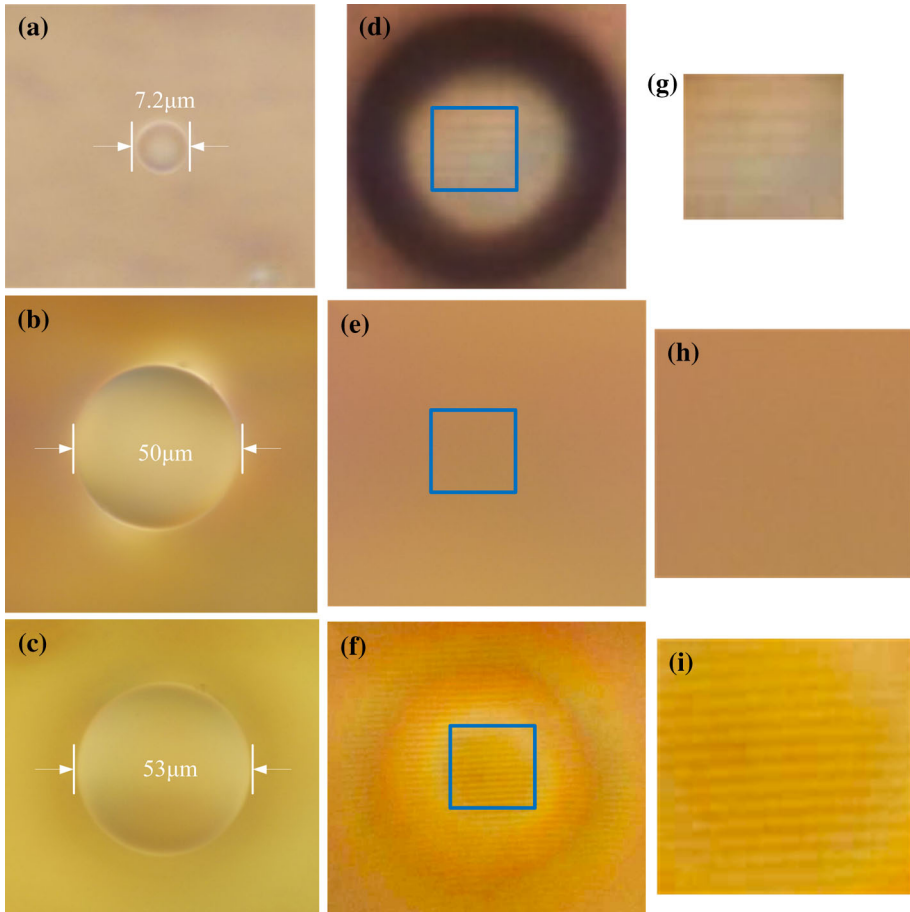
Fig. 10 Images of a grating with nanostructure by microspheres with different radius and refractive index. **a–i** Optical microscopy images obtained by SiO_2 microspheres with radius of 3.6 μm (**a, d, g**), 25 μm (**b, e, h**) and $BaTiO_3$ microspheres with radius of 26.5 μm (**c, f, i**), respectively. The images of **a–c** are focused on the center plane of the microspheres, while the corresponding images (**d–f**) are focused on the virtual image plane. **g–i** the magnified *rectangle area* marked with *solid blue line* in **d–f**, respectively. (Color figure online)

The experimental results indicate that the resolution increases with decrease of radius. The sub-wavelength information of the grating was observed in Fig. 10f. Comparing the results of Fig. 10f and e, the experimental results indicate that the resolution increases with increase of refractive index. The experimental results are consistent with the theoretical analysis and numerical simulations. In the theory, the resolution by using SiO_2 microspheres with 25 μm radius can arrive at 135 nm, and the grating consisting of 140 nm wide lines can be distinguished. It is worth noting that simulation and experiment results show that the resolution is lower than theoretical analyses because of occurring Whispering Gallery Mode inside of the microspheres. So the grating consisting of 140 nm wide lines cannot be distinguished by using SiO_2 microspheres with 25 μm radius.

5 Conclusion

Microsphere-assisted optical microscopy can transform the evanescent waves from the surface of the sample into propagating waves. Because of the spherical symmetries, the resolution can be improved in all orientations and super-resolution imaging is realized. We develop the equations of the resolution and field of view in microsphere imaging system related to the radius and refractive index of microspheres. Then we divide into three groups for theoretical analysis, numerical simulation and experiment. Through the analysis the highest spatial frequency of the system, the resolution is obtained with different radius and different refractive index of microspheres. The resolution reduces quickly with the increase of the radius when the radius is less than 10 μm. The resolution reduces slowly with the increase of the radius when the radius is more than 10 μm. At the same time, the resolution increases with the increase of refractive index. The size of focus is analyzed by changing different values of radius and refractive index in simulation using the finite element method by COMSOL Multiphysics. The theoretical analyses have been verified by numerical simulations. The experimental results verified the super-resolution capability of the microsphere-assisted optical microscopy. The results are useful for the practical design of the microsphere-assisted optical microscopy.

References

Ben-Aryeh, Y.: Superresolution observed from evanescent waves transmitted through nano-corrugated metallic films. Appl. Phys. B **109**, 165–170 (2012)

Darafsheh, A.: Optical super-resolution and periodical focusing effects by dielectric microspheres, pp. 1–249. Ph.D. Dissertation, University of North Carolina at Charlotte (2013)

Darafsheh, A., Walsh, G.F., Dal Negro, L., Astratov, V.N.: Optical super-resolution by high-index liquid-immersed microspheres. Appl. Phys. Lett. **101**, 141128 (2012)

Darafsheh, A., Limberopoulos, N., Derov, J.S., Walker, D.E., Astratov, V.N.: Advantages of microsphere-assisted super-resolution imaging technique over solid immersion lens and confocal microscopies. Appl. Phys. Lett. **104**, 061117 (2014)

Darafsheh, A., Guardiola, C., Nihalani, D., Lee, D., Finlay, J.C., Cárabe, A.: Biological super-resolution imaging by using novel microsphere-embedded coverslips. Proc. SPIE **9337**, 933705 (2015a)

Darafsheh, A., Guardiola, C., Palovcak, A., Finlay, J.C., Cárabe, A.: Optical super-resolution imaging by high-index microspheres embedded in elastomers. Opt. Lett. **40**, 5–8 (2015b)

Devilez, A., Stout, B., Bonod, N., Popov, E.: Spectral analysis of three-dimensional photonic jets. Opt. Express **16**, 14200–14212 (2008)

Durant, S., Liu, Z., Steele, J.M., Zhang, X.: Theory of the transmission properties of an optical far-field superlens for imaging beyond the diffraction limit. J. Opt. Soc. Am. B **23**, 2383–2392 (2006)

Hao, X., Kuang, C., Liu, X., Zhang, H., Li, Y.: Microsphere based microscope with optical super-resolution capability. Appl. Phys. Lett. **99**, 203102 (2011)

Inouye, Y., Kawata, S.: Near-field scanning optical microscope with a metallic probe tip. Opt. Lett. **19**, 159–161 (1994)

Jacob, Z., Alekseyev, L.V., Narimanov, E.: Optical hyperlens: far-field imaging beyond the diffraction limit. Opt. Express **14**, 8247–8256 (2006)

Lee, S., Lin, L.: Rapid super-resolution imaging of sub-surface nanostructures beyond diffraction limit by high refractive index microsphere optical nanoscopy. Opt. Commun. **334**, 253–257 (2015)

Lee, S., Li, L., Ben-Aryeh, Y., Wang, Z., Guo, W.: Overcoming the diffraction limit induced by microsphere optical nanoscopy. J. Opt. **15**, 1–7 (2013a)

Lee, S., Li, L., Wang, Z., Guo, W., Yan, Y., Wang, T.: Immersed transparent microsphere magnifying sub-diffraction-limited objects. Appl. Opt. **52**, 7265–7270 (2013b)

Li, L., Guo, W., Yan, Y., Lee, S., Wang, T.: Label-free super-resolution imaging of adenoviruses by submerged microsphere optical nanoscopy. Light: Sci. Appl. **2**, 1–9 (2013)

Liu, Z., Durant, S., Lee, H., Pikus, Y., Fang, N., Xiong, Y., Sun, C., Zhang, X.: Far-field optical superlens. Nano Lett. **7**, 403–408 (2006)

Miklyaev, Y.V., Asselborn, S.A., Zaytsev, K.A., Darscht, M.Y.: Superresolution microscopy in far-field by near-field optical random mapping nanoscopy. Appl. Phys. Lett. **105**, 113103 (2014)

Pendry, J.B.: Negative refraction makes a perfect lens. Phys. Rev. Lett. **85**, 3966–3969 (2000)

Wang, Z., Guo, W., Li, L., Luk'yanchuk, B., Khan, A., Liu, Z., Chen, Z., Hong, M.: Optical virtual imaging at 50 nm lateral resolution with a white-light nanoscope. Nat. Commun. **2**, 1–6 (2011)

Yan, Y., Li, L., Feng, C., Guo, W., Lee, S., Hong, M.: Microsphere-coupled scanning laser confocal nanoscope for sub-diffraction-limited imaging at 25 nm lateral resolution in the visible spectrum. ACS Nano **8**, 1809–1816 (2014)